Liu, Yunfang; Zeng, Qingfeng; Feng, Zhiqiang; Cheng, Laifei; Li, Liangjun; Zhang, Litong
Numerical Analysis of the Microstructure-based Model for Layered Composites via MC
and FEM Approaches
Brazilian Journal of Physics, vol. 46, núm. 1, febrero, 2016, pp. 87-96
Sociedade Brasileira de Física
Sâo Paulo, Brasil

GENERAL AND APPLIED PHYSICS

# Numerical Analysis of the Microstructure-based Model for Layered Composites via MC and FEM Approaches

Yunfang Liu[1] · Qingfeng Zeng[1,4] · Zhiqiang Feng[2,3,4] · Laifei Cheng[1,4] · Liangjun Li[1] · Litong Zhang[1]

**Abstract** A numerical approach combining the Monte Carlo (MC) and the finite element method (FEM) is developed and applied to investigate the mechanical performance of layered composites. We consider a simplified two-dimensional layered composite model and mainly focus on the stress response with the effects of the grain orientation, grain boundary properties, and the laminated topological structure. The stress distribution in the materials is heterogeneous in each individual layer because of grain orientation. The stress level in the hard layers is higher than that in the soft layers from the point of view of global stress distribution. The average stress changes with the inner layer thickness and the number of layers. The average stress increases almost linearly with the modulus ratio for the homogeneous materials, whereas it is nonlinear for the heterogeneous polycrystalline layered materials.
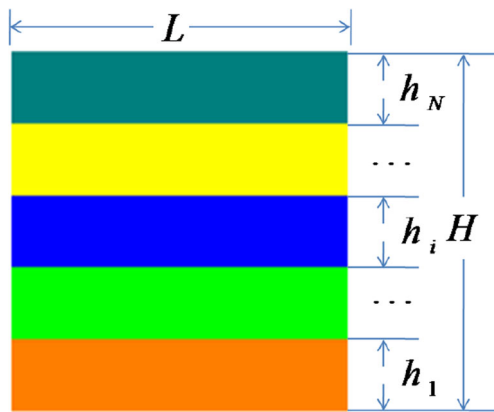
✉ Qingfeng Zeng
qfzeng@nwpu.edu.cn

1   Science and Technology on Thermostructural
    Composite Materials Laboratory, School of Materials Science
    and Engineering, Northwestern Polytechnical University,
    Xi'an, Shaanxi 710072, People's Republic of China

2   School of Mechanics and Engineering,
    Southwest Jiaotong University, Chengdu, Sichuan 610031,
    People's Republic of China

3   Laboratoire de Mécanique et d'Energétique,
    Université d'Evry, Evry 91020, France

4   International Center for Materials Discovery,
    School of Materials Science and Engineering, Northwestern
    Polytechnical University, Xi'an, Shaanxi 710072,
    People's Republic of China

## 1 Introduction

Layered composites, especially layered ceramics, are considered to be a very promising material for different engineering applications because of their excellent mechanical properties such as high hardness, high strength, and high fracture toughness, instead of a catastrophic fracture behavior like monolithic ceramics. Therefore, many experimental studies have focused on manufacturing materials with optimal properties by designing different compositions and alternative geometry parameters including the number of layers and the layer thickness ratios [1–5]. Usually, the layered ceramics can be prepared by several methods: tape casting, slip casting, rolling, and extrusion, followed by sintering. Generally speaking, the obtained materials are homogeneous in each individual layer in a macroscale but are polycrystalline in a microscale. As we know, the grain structure is an important microstructural feature of a material, which will greatly affect the mechanical properties such as strength and toughness. During the last few decades, many researchers have made great efforts in the study of microstructure evolution by numerical simulation methods such as cellular automaton [6, 7], phase field [8], and Monte Carlo (MC) [9] methods.

At present, the MC method is one of the most popular methods owing to its simplicity and flexibility and has been applied to obtain the microstructure evolution [10–14]. Anderson and Srolovitz [15, 16] first applied the Potts model to simulate the two-dimensional grain growth. Currently, the MC method and the modified MC method

**Fig. 1** A section illustration of typical multilayered composite materials

have been widely used in the simulation of solid-state sintering process for ceramic tool materials [17–19]. In addition, Guan et al. [20] built a geometrical tricrystal model with one cavity at the point where three crystal boundaries intersect and analyzed the stress distribution of the polycrystalline material by using the finite element method (FEM) software ABAQUS. Vedula et al. [21] predicted the residual stresses in polycrystalline alumina samples using experimentally determined grain orientations and object-oriented finite element analysis. A micro-macro method based on MC and FEM was proposed by Mori et al. [22] to simulate a

sintering process of ceramic powder compacts. However, the underlying microstructure morphology is often neglected in simulation of layered composites. In our previous work [23], the numerical simulation was successfully applied by combining MC and FEM to perform the stress analysis of the polycrystalline materials during the microstructure evolution, and we found that the average stress and the grain size agree well with the Hall-Petch relation when the properties of the grain boundaries are taken into account.

The present study aims to investigate the mechanical performance of layered composites, together with polycrystalline microstructures and alternative geometry parameters. After a brief description of the computational methods about MC techniques and finite element method in Section 2, we show the calculated results including microstructure evolution of grain growth and the stress distribution of layered materials in Section 3. The main conclusions are presented in Section 4.

## 2 Simulation Methods

In this paper, we consider a layered composite consisting of $N$ layers that are alternatively designed and perfectly bonded at the interfaces. For the sake of simplicity, a 2D problem is involved here, and the schematic of layered materials is shown in Fig. 1.

**Fig. 2** Flow chart of MC simulation for microstructure evolution
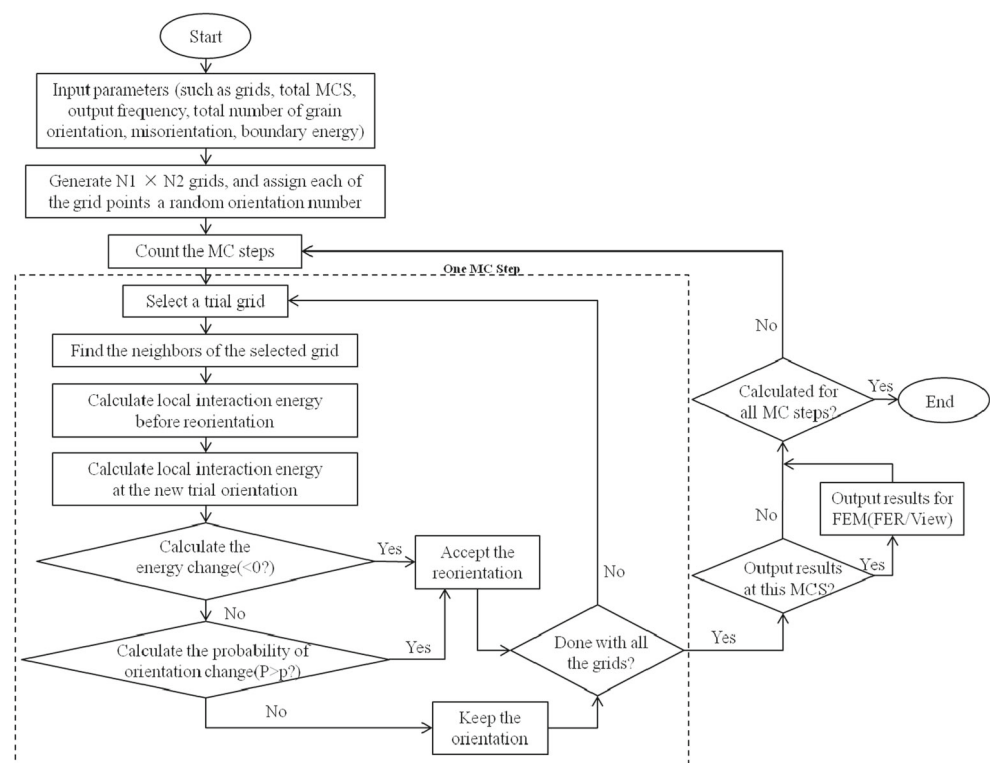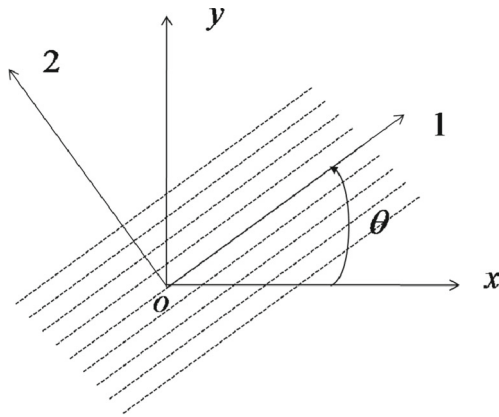
**Fig. 3** Grain orientation [23]

## 2.1 Monte Carlo Simulation

In the MC approach for microstructure evolution simulation, a 2D continuum microstructure is mapped onto a discretized domain that composes a set of $N_1 \times N_2$ square lattice grids.

The state of the lattice grid is represented by a random orientation number $q$ between 1 and the total orientation number $Q$. In this paper, the value of $Q$ is 48, so the orientation angle between two grains above 7.5° can be distinguished. There are eight neighbors including the second nearest ones at most for each lattice grid. The adjacent lattice grid with the same state will form a grain. The grain area, $A$, is the number of lattice grids within one grain. The grain size ($R$) and the mean grain size ($\langle R \rangle$) are defined by $R = \sqrt{A}$ and $\langle R \rangle = \sqrt{\frac{N}{N_{\text{grain}}}}$ [24], respectively, where, $N$ is the total number of lattice grids, and $N_{\text{grain}}$ is the number of grains of the microstructure.

During the microstructure evolution, the grain boundary migration is driven by the local interaction energy variation $\Delta E$ with a probability of reorientation $P$, which is defined as

$$P = \begin{cases} 1, & \Delta E \leq 0 \\ \exp\left(-\Delta E / k_{\text{B}} T\right), & \Delta E > 0 \end{cases}, \tag{1}$$

where $k_{\text{B}}$ is the Boltzmann constant, and $T$ is the temperature. The local interaction energy, $E_{\text{loc}}$, as a function of the grain misorientation across the boundary is calculated using
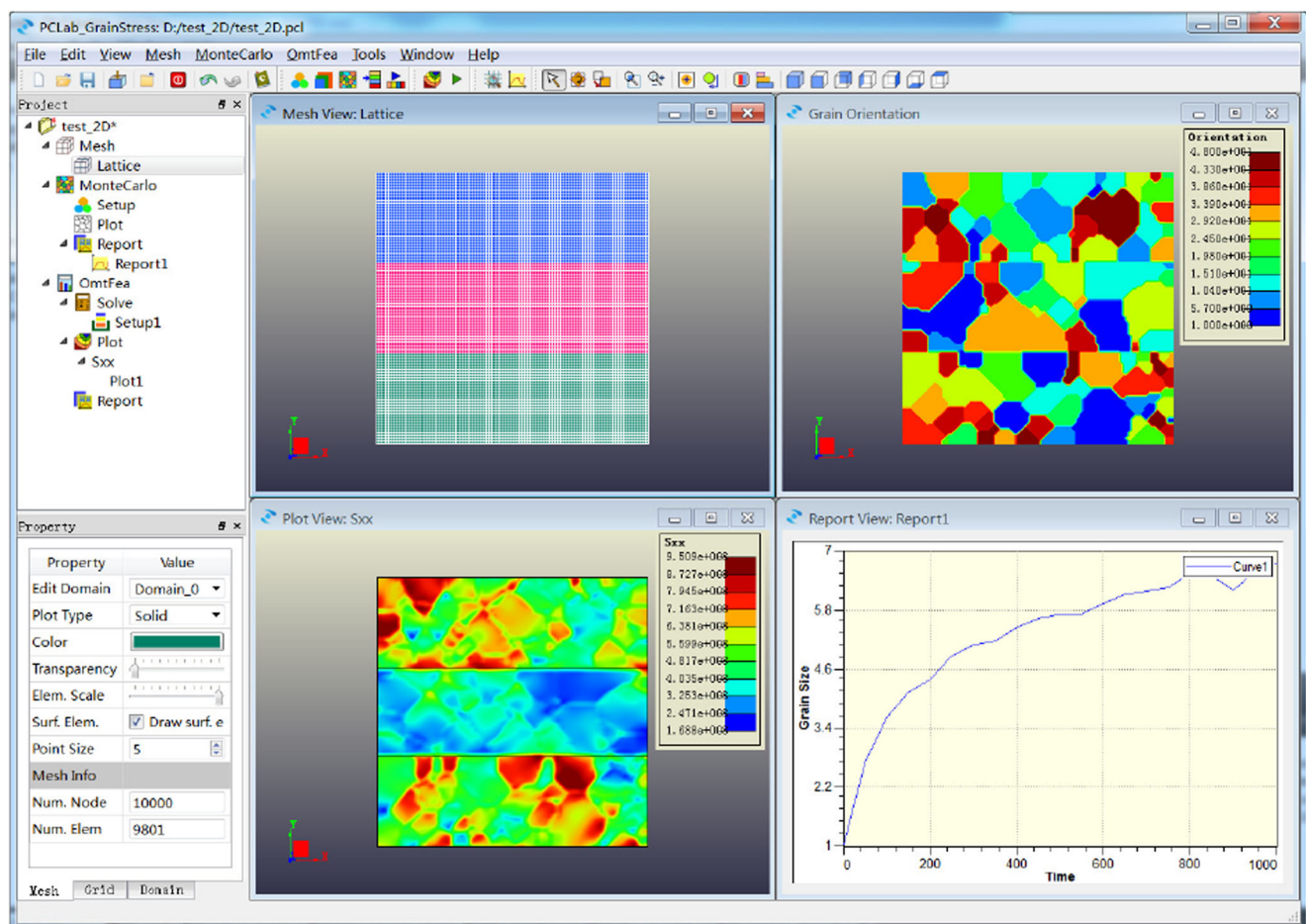


**Fig. 4** A GUI of PCLab/GrainStress software package
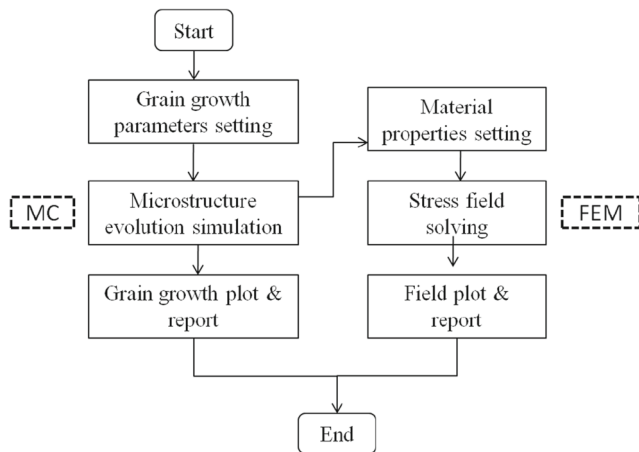
**Fig. 5** Flow diagram of the software

the Hamiltonian, which sums the interfacial energy of the neighbor grids:

$$E_{\text{loc}} = \sum_{j=1}^{n} V(1 - \delta_{q_i q_j}), \tag{2}$$

where $\delta$ is the Kronecker's delta function, $q_i$ and $q_j$ denotes the orientation number of the neighboring grids $i$ and $j$, and $n$ is the total number of the nearest neighbor grids. The grain boundary energy $V$, derived by Read and Shockley [25], is specified by defining an interaction between nearest neighbor grids, and it depends on the misorientation parameter, $\theta^*$, above which grain boundaries are considered to be high angle and a positive constant, $J$, which sets the scales of the grain boundary energy. $V(\theta)$ is given as follows:

$$V(\theta) = \begin{cases} J \frac{\theta'}{\theta^*}[1 - \ln(\frac{\theta'}{\theta^*})], & \theta' < \theta^* \\ J, & \theta' \geq \theta^* \end{cases} \tag{3}$$

where $\theta' = \begin{cases} |\theta|, & 0 \leq |\theta| \leq \pi \\ 2\pi - |\theta|, & \pi \leq |\theta| \leq 2\pi \end{cases}$, $\theta = 2\pi(q_i - q_j)/Q$

More details on MC technique can be found in our previous paper [23]. The energy gradient due to the mismatches in Young's modulus and thermal gradients would also affect the grain size distribution. In order to simplify the assumptions, these contributions are not to be included in the MC model.

Figure 2 shows the flow chart of MC simulation for microstructure evolution. The simulation time is measured in terms of a Monte Carlo step (MCS). Each MCS repeats the procedure to judge the reorientation attempts for all the $N_1 \times N_2$ lattice grids.

## 2.2 Finite Element Analysis

For the sake of simplicity, a cross section of a linearly elastic material is taken into account. The fundamental equations

of elasticity theory including equilibrium equations, kinematics equations, and constitutive equations, which have been described in detail in Ref. [23], are applied for the numerical computation of mechanical behaviors of layered composites. A plane strain problem neglecting body forces is considered here. The 2D finite element model corresponding to the microstructure is utilized for the numerical mechanical analysis. The four-node linear element is used in the analysis, and the nodes correspond to the grids obtained by the MC technique. The finite element equation is shown as follows:

$$\boldsymbol{Ku} = \boldsymbol{P}, \tag{4}$$

where $\mathbf{u}$ is the unknown vector of global nodal displacement, $\mathbf{K}$ is the global stiffness matrix assembled by the element stiffness matrix $\mathbf{K^e}$, and $\mathbf{P}$ is the global load vector. The element stiffness matrix $\mathbf{K^e}$ is given by

$$\boldsymbol{K^e} = \int_{V_e} \boldsymbol{B^T D B} \mathrm{d}\mathbf{V}, \tag{5}$$

where $\mathbf{B}$ is the strain matrix, and $\boldsymbol{D}$ is the elasticity matrix, which will be transformed by taking into account the grain orientation. Supposing $\mathbf{D}$ and $\mathbf{D}'$ represent elastic tensors in the global coordinate system and the local coordinate system, respectively, the following can be obtained $\mathbf{D} = \mathbf{Q}^T \mathbf{D}' \mathbf{Q}$, where $\mathbf{Q}$ is the transformation matrix written as [26]

$$\boldsymbol{Q} = \begin{bmatrix} l_1^2 & m_1^2 & n_1^2 & 2l_1 m_1 & 2m_1 n_1 & 2n_1 l_1 \\ l_2^2 & m_2^2 & n_2^2 & 2l_2 m_2 & 2m_2 n_2 & 2n_2 l_2 \\ l_3^2 & m_3^2 & n_3^2 & 2l_3 m_3 & 2m_3 n_3 & 2n_3 l_3 \\ l_1 l_2 & m_1 m_2 & n_1 n_2 & l_1 m_2 + l_2 m_1 & m_1 n_2 + m_2 n_1 & n_1 l_2 + n_2 l_1 \\ l_2 l_3 & m_2 m_3 & n_2 n_3 & l_2 m_3 + l_3 m_2 & m_2 n_3 + m_3 n_2 & n_2 l_3 + n_3 l_2 \\ l_3 l_1 & m_3 m_1 & n_3 n_1 & l_3 m_1 + l_1 m_3 & m_3 n_1 + m_1 n_3 & n_3 l_1 + n_1 l_3 \end{bmatrix} \tag{6}$$
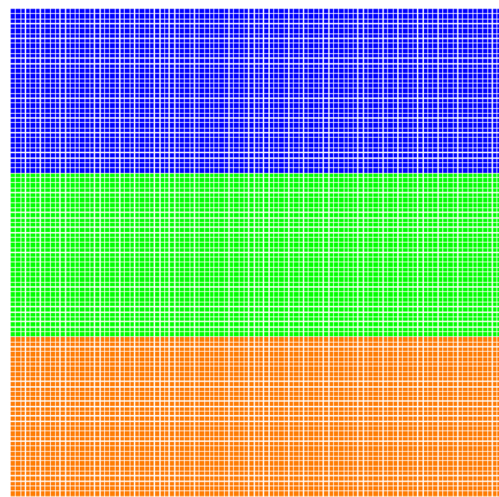


**Fig. 6** Mesh of a three-layered composite with layer thickness ratio of 1:1:1

**Fig. 7** Overview of the layered structures: **a** homogeneous—without boundary and **b** heterogeneous—with boundaries between grains
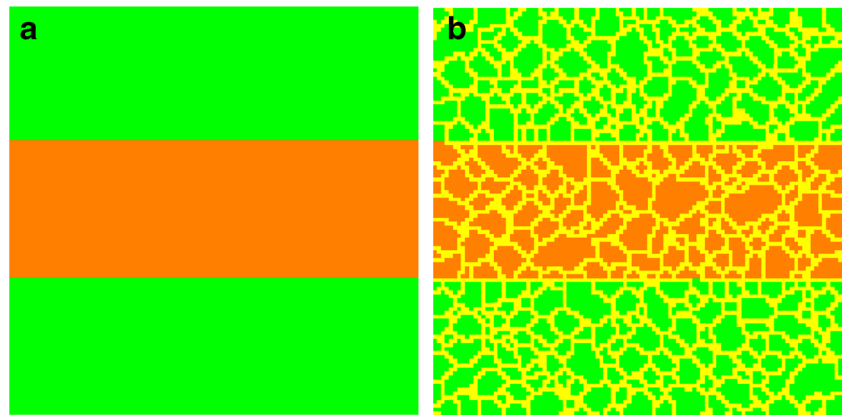


with $l_i$, $m_i$, $n_i$ being directional cosines of three axes of the local coordinate system with respect to the global coordinate system. In the manuscript, let $oxy$ be a global coordinate system and $o12$ be a local coordinate system, and the grain orientation $\theta$ is shown in Fig. 3 in two dimensions, and the transformation matrix for the 2D finite element model is [23]:

$$Q = \begin{bmatrix} \cos^2\theta & \sin^2\theta & 2\sin\theta\cos\theta \\ \sin^2\theta & \cos^2\theta & -2\sin\theta\cos\theta \\ -\sin\theta\cos\theta & \sin\theta\cos\theta & \cos^2\theta - \sin^2\theta \end{bmatrix}. \quad (7)$$

with $\theta$ being the orientation angle.

The mechanical properties of microheterogeneous materials are characterized by a spatially variable elasticity tensor $C$. Typically, to characterize the homogenized effective macroscopic response of such materials, a relation between averages is given by

$$\langle\sigma\rangle = C^* : \langle\varepsilon\rangle, \quad (8)$$

where the quantity $C^*$ is the elasticity tensor defined within the domain $\Omega$. The average stress $\langle\sigma\rangle$ and the average strain $\langle\varepsilon\rangle$ are defined by

$$\langle\sigma\rangle = \frac{1}{|\Omega|}\int_\Omega \sigma \mathbf{d}\Omega, \qquad \langle\varepsilon\rangle = \frac{1}{|\Omega|}\int_\Omega \varepsilon \mathbf{d}\Omega. \quad (9)$$

## 3 Numerical Results and Discussion

The algorithms mentioned previously have been implemented into an in-house software platform OMT (Objected and Methodological Technology), and a software named PCLab/GrainStress (Particle Cloud Laboratory/Grain Stress) is especially developed to simulate the grain growth process using MC method and to perform stress analysis of the microstructure with FEM (Fig. 4). This software is written using the object-oriented programming language C++, and the flow diagram is shown in Fig. 5. There are mainly two procedures, namely the Monte Carlo simulation module and the finite element stress analysis module. After each MC step, the microstructure and the analysis data including grid orientations, mean grain size, number of grains, and simulation time (MCS) are recorded in files. The microstructure distributions are different at each MC step, and the grains grow larger as the simulation time as a whole. The structures with different microstructure distributions will exhibit different mechanical performance. So we investigated the stress distribution after finishing all the MC steps simulation. Several numerical tests are carried out to investigate the effects of the microstructure and the geometry parameters on the mechanical performance of layered materials. Part of the results is displayed by the postprocessing software FERView [27].

**Fig. 8** The microstructure evolution of a three-layer material obtained by MC: **a** 100 MCS, **b** 500 MCS and **c** 900 MCS
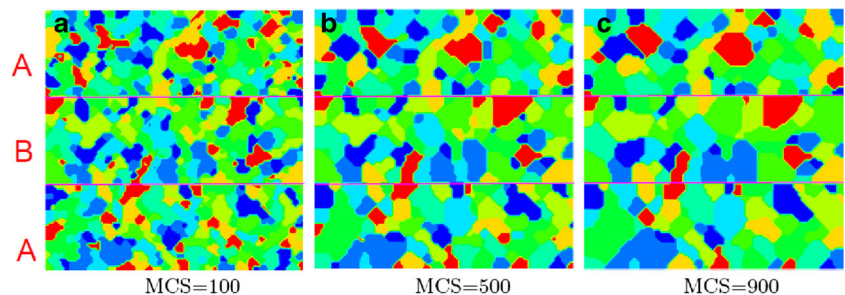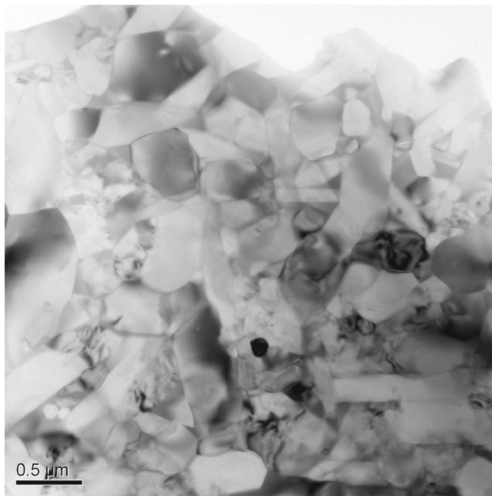
**Fig. 9** The TEM (transmission electron microscope) micrograph of $Si_3N_4$ layered material

### 3.1 The Layered Material Structure

For the multilayer composite materials (Fig. 1), the total thickness of specimen of rectangular cross section is $H = 0.01$ m, its total width is $L = 0.01$ m, and the total number of layers is $N$. The model is applied with a given displacement $u = 0.002$ L on the right boundary. $E_i$ and $v_i$ are the Young's modulus and Poisson ratio of the $i$th layer in macroscopic scale, respectively. In this work, the material to be considered consists of $N$ layers with alternative layers of A and B; $E_i = E_A$, $v_i = v_A$ for odd layer, and $E_i = E_B$, $v_i = v_B$ for even layer. For numerical tests, we assume that $E_A = 300$ GPa, $E_B = 150$ GPa, and $v_A = v_B = 0.2$. The four-node element, whose nodes are associated with the microstructure grids obtained by MC simulation, is applied in the stress analysis. Generally, the layered composites can be designed with different number of layers, different layer thickness ratio, and different layer thickness. Figure 6 shows the mesh of a three-layered composite with identical layer thickness.

Usually, there are relatively thin boundaries between grains in the materials. Thus, the overview of the layered material structure is shown in Fig. 7. Actually, the effects of grain boundary, such as strengthen or weaken effects, play important roles in the mechanical performance of the microstructure. In the finite element analysis, as proposed in the previous work [23], we considered a grain boundary between two grains and assigned it to be another material. The grain boundaries are composed of the elements whose nodes have different orientations. That is to say, if the orientations of the four nodes of an element are not the same, the

element belongs to a grain boundary. It is easy to assign the properties of the grain boundary, such as Young's modulus and Poisson's ratio, to study the effects of the grain boundaries. In this paper, we mainly focus on the stress response of a layered material with grain boundary (Fig. 7b), comparing that of a layered material with homogeneous layer (Fig. 7a). To view the simulation results quantitatively, the mean grain size and the average stress are calculated in the following subsections.

### 3.2 Microstructure Evolution of Grain Growth

For layered composites, it is assumed that the grains grow up independently in each individual layer, and the microstructure can be obtained layer by layer using MC simulation. The "pinning" of the grain boundaries to the
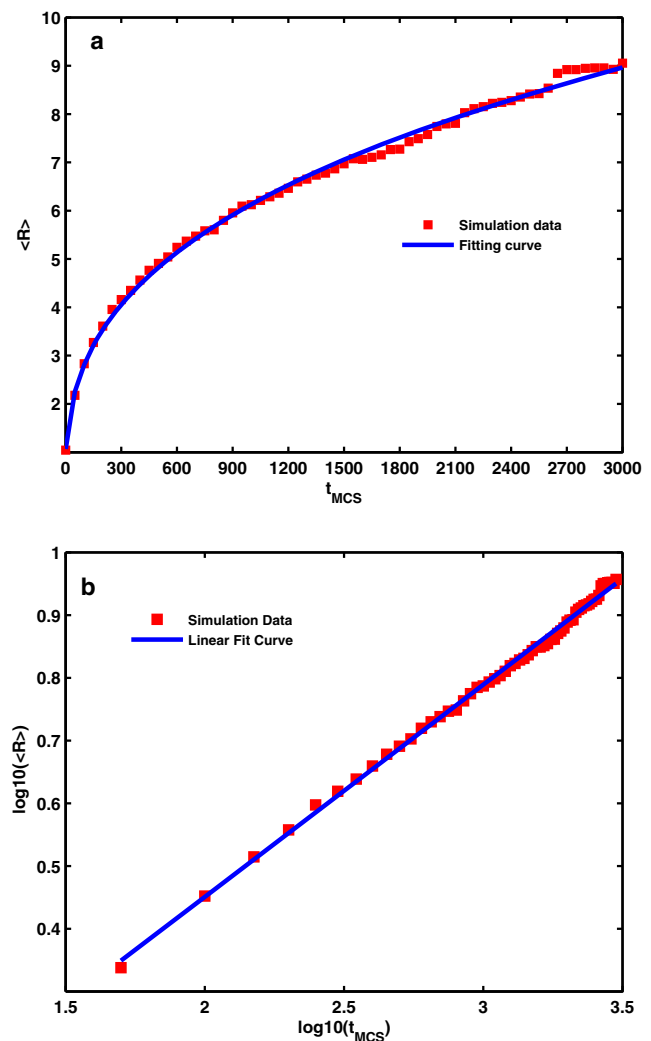


**Fig. 10** Mean grain size $\langle R \rangle$ vs. simulation time $t_{MCS}$: **a** $\langle R \rangle$-$t_{MCS}$ and **b** $\log10(\langle R \rangle)$-$\log10(t_{MCS})$

**Fig. 11** Stress distribution along the *x* direction of a three-layer material: **a** heterogeneous, MCS = 500, and **b** homogeneous
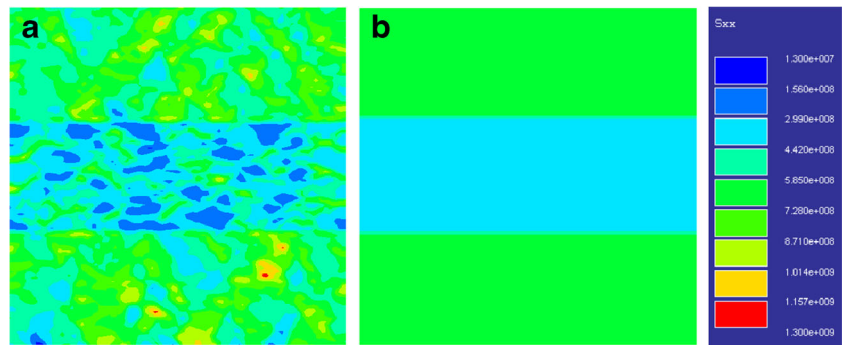


underlying lattice is an inherent feature common to all curvature driven, Q-state Monte Carlo methods. Since the effect is nonphysical, in practice, it has prompted the development of two primary mitigation strategies. The first method involves the augmentation of nearest neighbor interactions to include second-order interactions, and the second method involves an increase in the simulation temperature ($k_B T$) in order to activate thermal fluctuations that serve to provide numerical asperities along grain boundaries [28]. During the MC simulation in this study, a grid with second nearest neighbors is taken into account. A sintering temperature 1773 K is selected to the simulation temperature; the positive constant *J* is set to be 1 and 2 for the outer and inner layers, respectively; and $\theta^*$ is set to $0.3\pi$ and $0.4\pi$ for the outer and inner layers, respectively.

Microstructure evolution of grain growth of a three-layer material for different simulation times is shown in Fig. 8, where different color regions indicate the grains with different orientations. Figure 9 shows the micrograph of as-received $Si_3N_4$ layered material and numerous grains are easy to be recognized. The grain rotation coalescence can be found from the results, which was indicated in the previous work [23]. During the evolution, some grains significantly shrink, and some grains grow at the same time.

Figure 10 is the relationship between mean grain size $\langle R \rangle$ and simulation time $t_{MCS}$, which shows that the mean grain size increases from about 3.0 at 100 MCS to about 9.0 at 3000 MCS.

### 3.3 Stress Distribution of Microstructure-based Multilayer Composite Materials

Figure 11a shows the corresponding stress distribution along the *x* direction of a three-layer material, taking account of microstructure effects (see Fig. 8 obtained by MC techniques described in Subsection 2.1), whereas Fig. 11b shows that of a homogeneous material. It is obvious that the stress distribution in Fig. 11a is heterogeneous

in each individual layer because of grain orientation, but it is homogeneous in Fig. 11b without considering the grain orientation. In addition, the material is formed with alternative layers of the hard layer (with high modulus $E_A$) and the soft one (with low modulus $E_B$). It can be seen that from the global stress distribution point of view, the stress level in the hard layers is higher than that in the soft layers.

Figure 12 shows the average stress along the *x* direction versus the mean grain size of a layered material with grain boundary. The average stress linearly increases to the minus square root of the mean grain size when the modulus ratios are smaller than 2, and it coincides with the conclusion of polycrystalline materials with weaken boundary effect in the previous work [23]. The average stress decreases with the minus square root of the mean grain size, indicating with strengthen boundary effect when the modulus ratios are larger than 2.
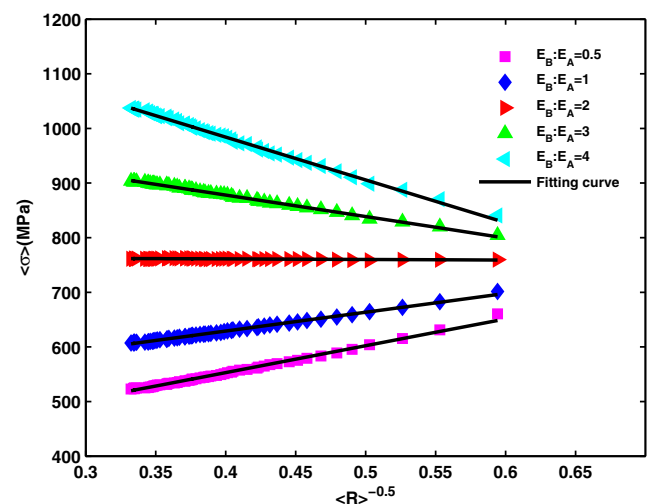


**Fig. 12** Average stress along the *x* direction vs. the mean grain size of a three-layer material with grain boundary for different modulus ratios

**Fig. 13** Stress distribution along the $x$ direction of a three-layer material with different thickness ratios: **a** 1:2:1 and **b** 2:1:2
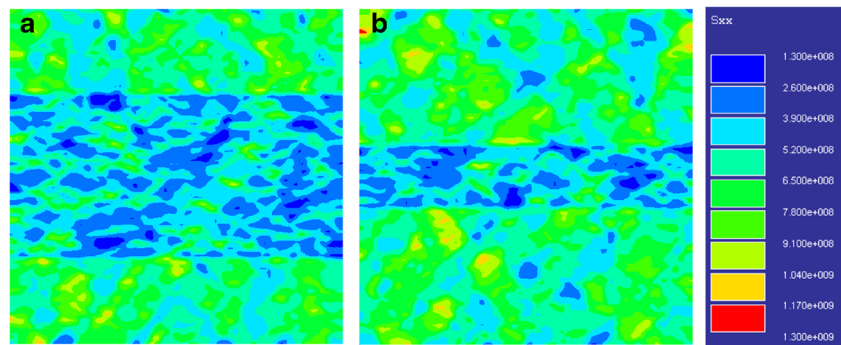


### 3.4 The Effects of the Geometry Parameters on the Mechanical Performance

#### 3.4.1 The Effects of Different Layer Thickness Ratio

Two different kinds of layer thickness ratios of a three-layer material, 1:2:1 and 2:1:2, are considered here. Figure 13 shows the corresponding stress distribution along the $x$ direction with the above-specified layer thickness ratios. The stress distributions are both heterogeneous in these two materials, and the magnitudes are different with each other. For the former case, the maximum and minimum stresses are about 1.15 GPa and 140 MPa, respectively. For the latter case, the maximum and minimum stresses are about 1.25 GPa and 172 MPa, respectively.

The average stress along the $x$ direction versus four kinds of layer thickness ratios (2:1:2, 1:1:1, 1:2:1, and 1:3:1) for the materials with different modulus ratios ($E_B : E_A = \frac{1}{5}, \frac{1}{2}, 1, 2, 3, 4$) is shown in Fig. 14. Notice that the average stress increases with the inner layer thickness when the modulus ratios are above 2, whereas the average stress decreases with the inner layer thickness when the modulus ratios are below 1. This is the result of the volumetric effect of the hard layer(s) in the composite materials.

#### 3.4.2 The Effects of the Different Number of Layers

Four kinds of layer number, 3, 5, 7, and 9, are considered here. The corresponding stress distributions along the $x$ direction with two kinds of layer number, 5 and 7, are shown in Fig. 15. The microstructure distributions are different at each MC step, and the grains grow larger as the simulation time as a whole. The structures with different microstructure distributions will exhibit different mechanical performance. After finishing all the MC steps simulation, we investigated the stress distribution. We imported the input data for the FEM model from the files which are built in MC procedures, calculated the stress distribution for each output MCS, and obtained the average stress along the $x$ direction. Then, we

plot the results, and the relation between the average stress versus simulation time is obtained. Figure 16 with two sub-figures shows the average stress along the $x$ direction versus the simulation time for the materials with four different layers. These two subfigures represent the two cases of different stacking sequence. It can be indicated that the average stress decreases with simulation time, no matter what the stacking sequence is. For the case of the outer hard layer, the stress decreases with the number of layers (Fig. 16a), whereas it increases for the case of the outer soft layer (Fig. 16b).

#### 3.4.3 The Effects of Different Modulus Ratios

The modulus ratios of inner layer to outer layer, nine case studies in total, are set, that is, 1:5, 1:4, 1:3, 1:2, 1:1, 2:1, 3:1, 4:1, and 5:1 for each test, whereas other features remain unchanged. The results of the simulation are presented in Fig. 17, where the average stress-modulus ratio curves of
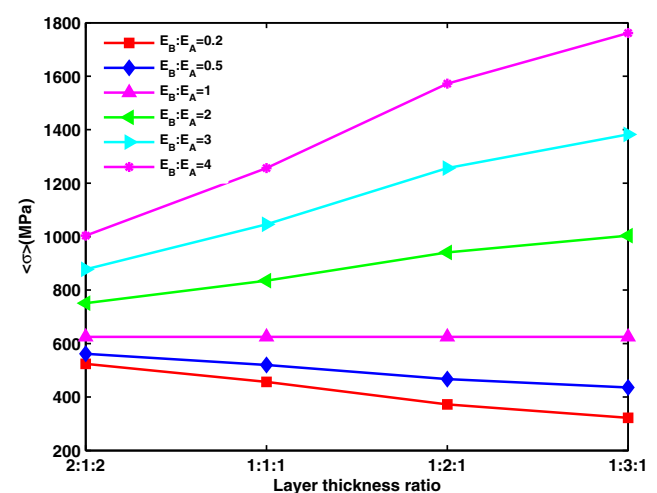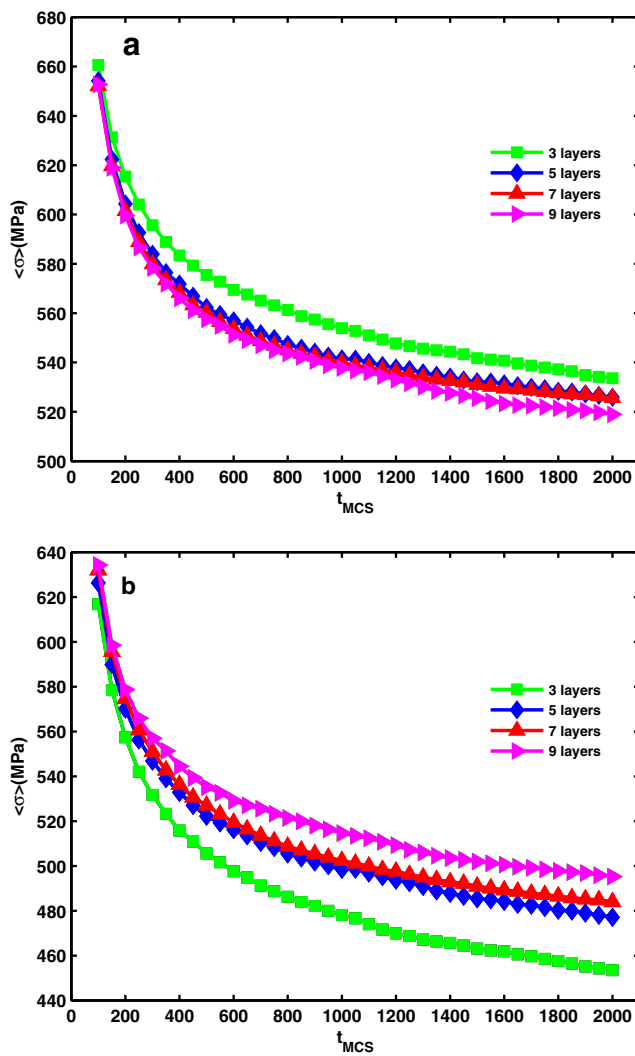


**Fig. 14** Average stress along the $x$ direction vs. layer thickness ratio for the materials with different modulus ratio $E_B : E_A$ (keep $E_A$, $E_B : E_A = \frac{1}{5}, \frac{1}{2}, 1, 2, 3, 4$)

**Fig. 15** Stress distribution along the $x$ direction of a layered material with different number of layers (considering grain boundaries): **a** five layers and **b** seven layers
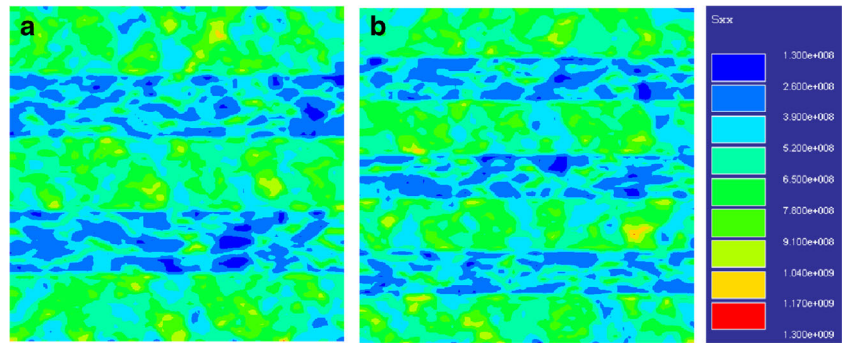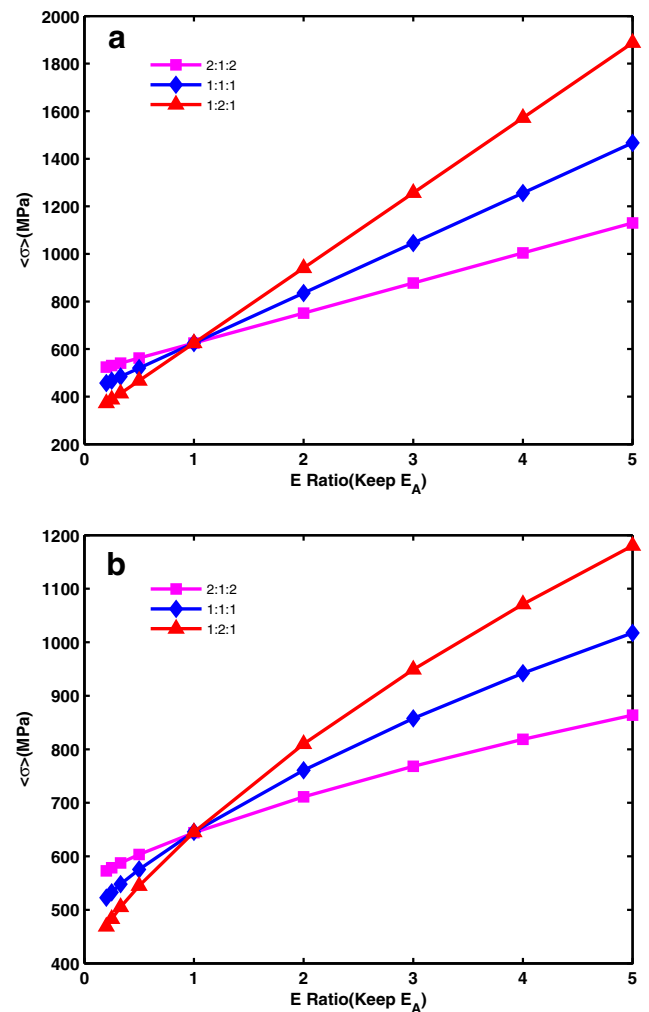


homogeneous and heterogeneous layered materials are plotted in Figs. 17a, b, respectively. From these figures, it is clear that the average stress increases almost linearly with respect to modulus ratios for homogeneous materials, whereas it is nonlinear for materials with heterogeneous microstructures. The average stresses in the heterogeneous



**Fig. 16** Average stress along the $x$ direction vs. simulation time for the materials with grain boundary with different layers: **a** hard outer layer and **b** soft outer layer. The thicknesses of the outer and inner layers are identical

**Fig. 17** Average stress along the $x$ direction vs. modulus ratio $E_B : E_A$ for materials with different layer thickness ratio (keep $E_A$, $E_B : E_A = \frac{1}{5}, \frac{1}{4}, \frac{1}{3}, \frac{1}{2}, 1, 2, 3, 4, 5$): **a** homogeneous and **b** heterogeneous, MCS = 500

composite materials are lower than those of the homogeneous ones in some cases. For example, the average stress of the homogeneous composite material with the layer ratio of 1:1:1 and the modulus ratio of 5 is more than 1400 MPa, while the average stress of the heterogeneous one with the same layer thickness is about 1000 MPa. That is mainly caused by the grain boundaries and the grain orientation.

## 4 Conclusions

A grain growth simulation with MC and a microstructure-based FEM approaches have been presented for two-dimensional mechanical analysis of layered composites. The microstructure evolution and the stress distribution have been analyzed in terms of the mean grain size and the average stress of layered materials. The grains nonlinearly grow with the MCS. The stress distribution in the materials is heterogeneous in each individual layer because of grain orientation, and the stress level in the hard layers is higher than that in the soft layers from the global stress distribution point of view. The average stress increases with the inner layer thickness when the modulus ratios are above 2, whereas it decreases when the modulus ratios are below 1. For the case of the outer hard layer, the stress decreases with the number of layers, whereas it increases for the case of the outer soft layer. The average stress increases almost linearly as modulus ratios for the homogeneous material, whereas it is nonlinear to the modulus ratios for the materials with heterogeneous microstructures. It is therefore possible to tune the stress distribution by varying the grain size, the layer thickness ratio, the number of layers, and the modulus ratios. A software package, PCLab/GrainStress, for the grain growth process and stress analysis will provide an efficient tool for faster material design and application.

## References

1. R. Bermejo, A.J. Sánchez-Herencia, L. Llanes, C. Baudín, Acta Mater. **55**(14), 4891 (2007)
2. R. Bermejo, J. Pascual, T. Lube, R. Danzer, J. Eur, Ceram. Soc. **28**(8), 1575 (2008)
3. C.W. Li, C.A. Wang, Y. Huang, Rare Metal Mater. Eng. **34**, 475 (2005)
4. Z. Yang, S. Sista, J.W. Elmer, T. Debroy, Acta Mater. **48**(20), 4813 (2000)
5. Q. Yu, S.K. Esche, Mater. Lett. **57**(30), 4622 (2003)
6. J. Geiger, A. Roósz, P. Barkóczy, Acta Mater. **49**(4), 623 (2001)
7. D.S. Svyetlichnyy, Sci, Modell. Simul. Mater. Eng. **22**(8), 085001 (2014)
8. C.E. Krill, III, L.Q. Chen, Acta Mater. **50**(12), 3057 (2002)
9. P. Blikstein, A.P. Tschiptschin, Mater. Res. **2**, 133 (1999)
10. S.M. Hafez Haghighat, A. Karimi Taheri, Mater. Des. **28**(9), 2533 (2007)
11. A. Brahme, J. Fridy, H. Weiland, A.D. Rollett, Modell. Simul. Mater. Sci. Eng. **17**(1), 015005 (2009)
12. L. Sieradzki, L. Madej, Comp. Mater. Sci. **67**, 156 (2013)
13. S.K. Esche, Monte Carlo simulations of grain growth in metals (InTech, 2011), pp. 581–610
14. J.B. Allen, C.F. Cornwell, B.D. Devine, C.R. Welch, Comp. Mater. Sci. **71**, 25 (2013)
15. M.P. Anderson, D.J. Srolovitz, G.S. Grest, P.S. Sahni, Acta Metall. **32**(5), 783 (1984)
16. D.J. Srolovitz, M.P. Anderson, P.S. Sahni, G.S. Grest, Acta Metall. **32**(5), 793 (1984)
17. H.M. Cheng, C.Z. Huang, H.L. Liu, B. Zou, Comp. Mater. Sci. **47**(2), 326 (2009)
18. B. Fang, C.Z. Huang, H.L. Liu, C.H. Xu, S. Sun, J. Mater, Process. Technol. **209**(9), 4568 (2009)
19. S. Hao, C.Z. Huang, B. Zou, J. Wang, H.L. Liu, H.T. Zhu, Comp. Mater. Sci. **50**(12), 3334 (2011)
20. X. Guan, X.L. Geng, Northwest. Polytech. J. Univ. **22**(6), 726 (2004)
21. V.R. Vedula, S.J. Glass, D.M. Saylor, G.S. Rohrer, W.C. Carter, S.A. Langer, E.R. Fuller, J. Am. Ceram. Soc. **84**(12), 2947 (2001)
22. K. Mori, H. Matsubara, N. Noguchi, Int. J. Mech. Sci. **46**(6), 841 (2004)
23. Y.F. Liu, L.F. Cheng, Q.F. Zeng, Z.Q. Feng, J. Zhang, J.H. Peng, C.W. Xie, K. Guan, Mater. Des. **55**, 740 (2014)
24. Q. Yu, M. Nosonovsky, S.K. Esche, Int. J. Mech. Sci. **51**(6), 434 (2009)
25. G.S. Grest, D.J. Srolovitz, M.P. Anderson, Acta Metall. **33**(3), 509 (1985)
26. Y.J. Xu, W.H. Zhang, H.B. Wang, Mater. Sci. Technol. **24**(4), 435 (2008)
27. Z.Q. Feng, Z.G. Feng, Computational mechanics. in *WCCM VI in conjunction with APCOM04*, ed. by Z.H. Yao, M.W. Yuan, W.X. Zhong (Springer, Beijing, China, 2004)
28. J.B. Allen, J. Eng. J. Eng. Mater.-T. ASME **136**(3) (2014)